*Materials Science-Poland, 31(3), 2013, pp. 471-475*
*http://www.materialsscience.pwr.wroc.pl/*
*DOI: 10.2478/s13536-013-0128-2*

VERSITA

# Investigation on multiferroic properties of $BiFeO_3$ ceramics

MOHAMMAD SHARIQ[1]*, DAVINDER KAUR[2], VISHAL SINGH CHANDEL[1], MOHD ASIM SIDDIQUI[1]

[1]Department of Physics, Integral University, Lucknow-226026, UP, India
[2]Functional Nanomaterials Research Laboratory, Department of Physics and Centre of Nanotechnology, Indian Institute of Technology, Roorkee 247667, India

$BiFeO_3$ polycrystalline ceramics was prepared by solid-state reaction method and its structural, optical and magnetic properties were investigated. $BiFeO_3$ was synthesized in a wide range of temperature (825 – 880 °C) and a well crystalline phase was obtained at a sintering temperature of 870 °C. X-ray diffraction patterns of the samples were recorded and analyzed for the confirmation of crystal structure and the determination of the lattice parameters. The average grain size of the samples was found to be between 1 – 2 μm. The determined value of direct bandgap of $BiFeO_3$ ceramics was found to be 2.72 eV. The linear behavior of M-H curve at room temperature confirmed antiferromagetic properties of the $BiFeO_3$ (BFO). *S* shaped M-H curve was obtained at a temperature of 5 K. In the whole temperature measurement range (5 – 300 K) of M-T, no anomalies were observed due to high Curie temperature and Neel temperature of the $BiFeO_3$.

Keywords: *$BiFeO_3$ ceramics; multiferroics; SQUID*



## 1. Introduction

In the last few years, the study of multiferroic compounds has undergone a large development. It has been largely due to the discovery of magneto-electric coupling, the appearance of electric polarization and low temperature magnetic phase transition in the materials which were not ferroelectric in their non-magnetically ordered state [1]. Despite a considerable interest in the fundamental understanding of multiferroic properties, these materials are of little applicability because of their weak magnetic/electric polarization and low temperatures at which these properties are observed. From this point of view, more "classical" multiferroics, i.e. ferroelectric compounds which tend to order magnetically, are now the subject of a renewed interest. They not only can be used in ferroelectric and magnetic devices [2] but also have the potential ability to couple electric and magnetic polarizations, providing an additional degree of freedom in device design and applications, such as in the emerging field of spintronics, [1] multiple state memory elements, [3] electric field controlled ferromagnetic resonance devices and transducers with magnetically modulated piezoelectricity [4]. Among all multiferroic materials studied so far, $ABO_3$-type perovskite structure $BiFeO_3$ (BFO) is a known Pb-free and environmentally friendly material. $BiFeO_3$ is ferroelectric ($T_C = 1100$ K), antiferromagnetic ($T_N = 643$ K) and exhibits weak magnetism at room temperature. It can be prepared as thin films and large crystals [5]. In addition to the potential magnetoelectric applications, BFO film might find other applications such as a photocatalytic compound [6] and in ultrafast optoelectronic devices due to its small bandgap ($E_g = 2.5$ eV) [7].

Due to the spiral magnetic structure with long wavelength (62 nm), even weak ferromagnetism, and consequently no linear magnetoelectric effect, should be observed in $BiFeO_3$. However, the linear magnetoelectric effect has been reported at large magnetic fields [8], chemical substitutions [9] and epitaxial strains in the case of $BiFeO_3$ thin films [10]. It was predicted that spontaneous magnetization can be induced in $BiFeO_3$ either by changing the Fe–O–Fe bond angle or by a statistical octahedral distribution of Fe with mixed

*E-mail: lucknow84iit@gmail.com

valence and chemical substitution [11]. In the case of thin films, however, it has been shown that heteroepitaxially strained BFO films become ferromagnetic at room temperature and show a remarkably large magnetoelectric coupling. In this research, a single-phase $BiFeO_3$ sample was synthesized by employing a rapid thermal processor to enhance the sintering rate. The structural, magnetic and optical properties of pure $BiFeO_3$ were investigated.

## 2. Experimental work

$BiFeO_3$ ceramics was prepared by conventional solid-state reaction with $Bi_2O_3$ and $Fe_2O_3$ as reactants. $Bi_2O_3$ and $Fe_2O_3$ powders with a purity of 99.9 % were mixed and grinded for 4 hours in an agate mortar followed by calcination at the temperature of 600 °C with a heating rate of 12 °C/min for 2 hours. In order to avoid an impurity phase of $Bi_2Fe_4O_9$ and unreacted $Bi_2O_3$ after calcination and sintering, an excess amount of $Bi_2O_3$ (10 wt.% extra) was added to the starting reactants. The powder was mixed with a few drops of 6 % concentrated aqueous polyvinyl alcohol (PVA) binder and again grinded in the agate mortar for 3 hours. Then, the mixed powder was pressed into different pellets at a pressure of $1.47 \times 10^8$ Pa. In order to evaporate the aqueous polyvinyl alcohol (PVA) binder, the pellets were heated at temperature of 250 °C for one hour. For optimizing the phases of $BiFeO_3$, the pellets were then sintered at 825 °C, 850 °C, 860 °C, 870 °C and 880 °C for 300 seconds. All the sintering processes were carried out in air and the sintering time was set to 300 sec.

Samples of $BiFeO_3$ ceramics sintered at different temperatures were characterized by the X-ray diffraction to confirm their phase formation. The microstructure of these samples was characterized by Bruker AXS D-8 advanced diffractometer with Cu K$\alpha$ radiation (1.54 Å) and step size of 0.02°. Energy dispersive X-ray analysis (EDAX) was carried out to determine the concentration of elements such as Bi, Fe, O in the sample of BFO. Magnetic properties were investigated by super conducting quantum interference device (SQUID, Quantum Design MPMS XL) magnetometer. Field emission scanning electron microscope (FEI Quanta 200F model) was used to determine the grain size and the uniformity of the synthesized $BiFeO_3$ samples. UV-VIS-NIR spectrometer (Varian Cary 5000 model) was used for optical characterization of the BFO.

## 3. Results and discussion

Fig. 1 shows the X-ray diffraction (XRD) patterns of $BiFO_3$ samples synthesized at different sintering temperatures (825 °C, 850 °C, 860 °C, 870 °C and 880 °C) to optimize their crystalline structure. XRD patterns demonstrate that impurity phases like $Bi_2Fe_2O_9$, $Bi_{25}FeO_{40}$ etc. were also formed along with $BiFeO_3$ phase and the intensity of these impurity phases decreased with increasing the temperature. Though the impurity phases were still observed in the diffraction patterns, their intensity had decreased greatly. When the sintering temperature was increased to 870 °C, the XRD pattern (Fig. 1) indicated the formation of single-phase $BiFeO_3$. Correspondingly, the pattern at 870 °C could exactly be indexed as $BiFeO_3$ according to the position and relative intensity of the diffraction peaks. Above the sintering temperature of 870 °C, formation of secondary phases started again, which can be attributed to melting of the sample resulting in decomposition of $Bi_{25}FeO_{40}$ and other secondary phases. The whole synthesis processing showed a critical role of sintering temperature in the formation of pure $BiFeO_3$ phase.

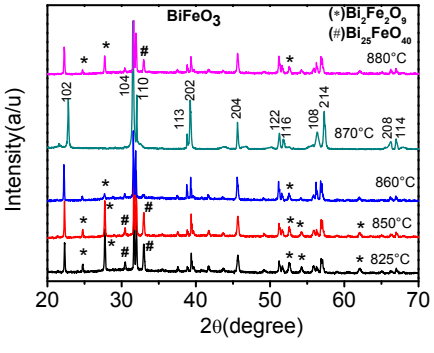


Fig. 1. XRD patterns of $BiFeO_3$ ceramics sintered at temperatures of 825 °C, 850 °C, 860 °C, 870 °C and 880 °C.

Room temperature lattice constant of BFO was calculated by the formula

$$\frac{1}{d^2} = \frac{(h^2+k^2+l^2)\sin^2\alpha + 2(hk+kh+hl)(\cos^2\alpha - \cos\alpha)}{\alpha^2(1-3\cos^2\alpha+2\cos^3\alpha)}. \quad (1)$$

We found the room-temperature lattice constants a = 5.626 Å and $\alpha = 59.351°$ in the rhombohedral cell of $BiFeO_3$. The lattice constant is slightly lower than that reported by Kubel and Schmid [12] while the rhombohedral angle agrees well within experimental uncertainties. These authors reported room temperature values of the lattice constants determined in a monodomain single crystal as a = 5.6343 Å and $\alpha = 59.348°$. The experimental uncertainties due to instrument calibration led to an error in peak position and correct positioning of the sample. The sample should be positioned exactly parallel to the surface of the sample holder.

SEM image shown in Fig. 2 reveals the fresh fracture section of the $BiFeO_3$ sample sintered at 870 °C. The SEM micrograph shows the uniform distribution of grains. It reveals average grain size of BFO of approximately 1 – 2 μm. Fig. 3 shows the atomic and weight percentage of BFO estimated by energy dispersive X-ray spectroscopy. The atomic percentages of the elements obtained by EDXS in the ceramic sample BFO are much closer to the actual values. Thus the EDXS analysis has verified the atomic and weight percentage of each element.

The optical absorption spectra of $BiFeO_3$ were recorded as a function of wavelength in the range of 300 – 900 nm and shown in the inset of Fig. 4. An absorption peak was found around 450 nm. Optical absorption at absorption edge corresponds to the transition from the valence band to conduction band, while the absorption in the visible region is related to some local energy levels caused by intrinsic defects. The reported values for the optical bandgap of $BiFeO_3$ at room temperature range from 2.3 to 2.8 eV [13–18]. According to some authors, this bandgap is direct [16, 17] although other reports suggest the presence of an indirect bandgap, of roughly 0.4 – 1.0 eV smaller than the direct one [14, 15]. Ab initio calculations using a screened exchange formalism show that bismuth

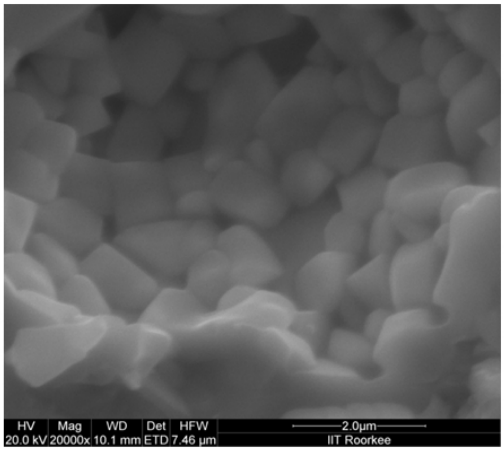


Fig. 2. SEM image of $BiFeO_3$ ceramics sintered at 870 °C.

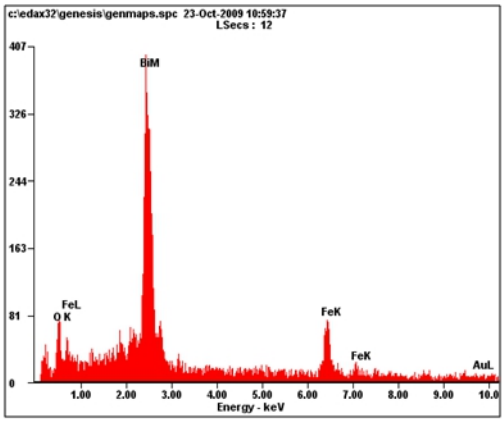


Fig. 3. EDXS results for $BiFeO_3$ sample.

ferrite is a semiconductor with a room-temperature gap of 2.8 eV [13, 18]. The valence-band maximum is at the R-point corner of the Brillouin zone, whereas the conduction-band minimum is at the center, G, so that the gap is indirect. However, the calculated valence band in the rhombohedral state is in fact almost flat [18], therefore the $BiFeO_3$ should behave in practice as a direct-bandgap semiconductor at room temperature.

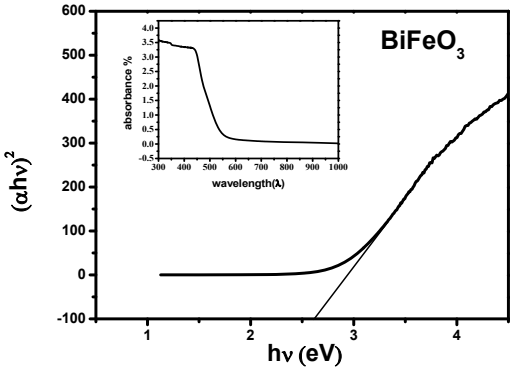


Fig. 4. Plot of $(\alpha h\nu)^2$ *vs.* photon energy $h\nu$ for the BFO. The direct bandgap energy is deduced from extrapolation of straight line to $(\alpha h\nu)^2 = 0$. The inset gives absorption spectra as a function of the wavelength.

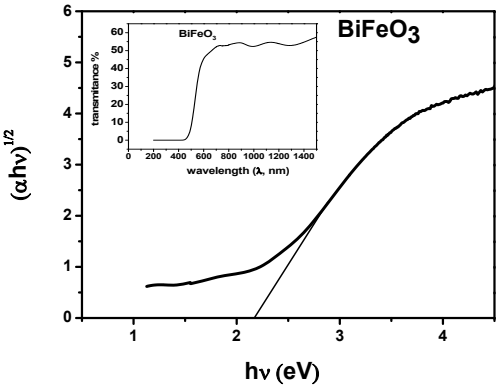


Fig. 5. Plot of $(\alpha h\nu)^{1/2}$ *vs.* photon energy $h\nu$ for the BFO for the determining of indirect bandgap. The inset gives transmission spectra as a function of the wavelength.

Tauc relationship [19] can be used to calculate energy bandgap

$$\alpha h\nu = A(h\nu - E_g)^n \qquad (2)$$

where $\alpha$ is the absorption coefficient, A is a constant, h is the Planck's constant, $\nu$ is the photon frequency, $E_g$ is the optical bandgap and $n$ is an index: $n = ½$ for allowed direct, $n = 2$ for allowed indirect, which dominates over the optical absorption. Fig. 4 shows the $(\alpha h\nu)^2$ versus $h\nu$ plot for the determination of direct optical bandgap. A linear behavior exists in a certain range, thus supporting the assumption of a direct bandgap transition. The inset in Fig. 5 shows the optical transmission spectra for the $BiFeO_3$ ceramics with variation of wavelength from 200 nm to 1500 nm. At the wavelength of 500 – 540 nm, the transmission of BFO decreases rather rapidly and finally approaches zero at around 450 nm. The fast decrease is due to absorption of light caused by the excitation of electrons from the valence band to conduction band of $BiFeO_3$. Indirect bandgap of $BiFeO_3$ has been also reported in some research papers as discussed earlier, so the indirect bandgap was evaluated by extrapolating the straight-line part of the curves $(\alpha h\nu)^{½} = 0$ as shown in Fig. 5. The determined value of direct bandgap of $BiFeO_3$ ceramics was found to be 2.72 eV, which is larger than indirect bandgap (2.22 eV) as confirmed by Gugar [14] and by Fruth et al. [15].

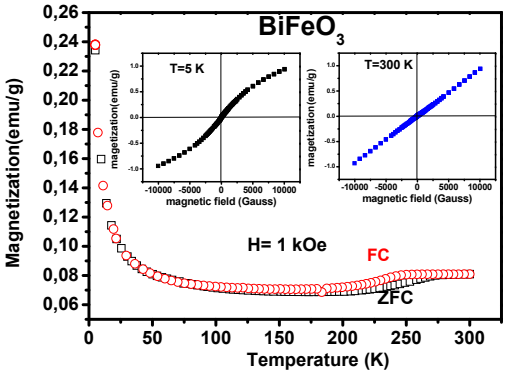


Fig. 6. Magnetization *vs.* temperature (M-T) for $BiFeO_3$ ceramics measured in an external field of 1 kOe. The insets show magnetization *vs.* external field (M-H) taken at 5 K and 300 K respectively.

The results of the magnetic measurements of $BiFeO_3$ samples obtained by solid state route are presented in Fig. 6. Magnetization of $BiFeO_3$ ceramics was measured in the external field of 1 kOe under field cooling (FC) and zero-field cooling (ZFC) conditions. Within experimental uncertainties the two magnetizations coincide, providing no evidence for spin-glass-like ordering. For temperatures below 200 K our results are roughly comparable to the reported by Lebeugle *et al.* for BFO single crystals [20]. The insets show magnetization measurements at 5 and 300 K indicating the absence of a ferromagnetic hysteresis within

experimental uncertainty. Microscopically, the antiferromagnetic spin order in $BiFeO_3$ single crystals is rather not homogeneous; an incommensurately modulated spin structure is present, which manifests itself as an incommensurate cycloid with long wavelength $\lambda \sim 600$ Å [21, 22]. Linear variation of magnetic moment with the magnetic field of pure $BiFeO_3$ at 300 K without opened hysteresis loop shows the antiferromagnetic nature of the BFO because the canted antiferromagnetic spins give rise to a net magnetic moment that is spatially averaged out to zero due to the cycloidal rotation. The weakly S-shaped magnetization at 5 K results from the presence of a small but finite amount of defect spins related to the upturn in the susceptibility at low fields and at the lowest temperatures [23].

## 4. Conclusions

Single phase of $BiFeO_3$ was obtained at an optimized sintering temperature of 870 °C. SEM micrographs revealed the average grain size of the ceramics of approximately 1 – 2 μm. Energy dispersive X-ray spectroscopy (EDXS) confirmed the atomic and weight percentage of each element. The determined value of direct bandgap of $BiFeO_3$ ceramics was found to be larger than that of indirect bandgap (2.22 eV). The linear variation of magnetic moment with magnetic field at room temperature confirmed the antiferromagnetic nature of the BFO. The magnetic anomalies were not observed below the room temperature and the phase transitions or glass transitions mentioned in some reports may have resulted from poor quality of the samples.

## References


[1] HUR N., PARK S., SHARMA P.A., AHN J.S., GUHA S., CHEONG S.W., *Nature* (2004), 392.
[2] CATALAN G. et al., *Phys. Rev. Lett.*, 100 (2008), 027602.
[3] WANG Y., NAN C. W., *Appl. Phys. Lett.*, 89 (2006), 052903.
[4] HILL N.A., *J. Phys. Chem. B*, 104 (2000), 6694.
[5] WANG J. et al., *Science*, 299 (2003), 1719.
[6] GAO F. et al., *Adv. Mater.*, 19 (2007), 2889.
[7] TAKAHASHI K., KIDA N., TONOUCHI M., *Phys. Rev. Lett.*, 96 (2006), 117402.
[8] POPOV Y. F., KADOMTSEVA A. M., VOROBEV G. P., ZVEZDIN A. K., *Ferroelectrics*, 162 (1994), 135.
[9] MURASHOV V. A., RAKOV D. N., IONOV V. M., DUBENKO I. S., TITOV Y. V., GORELIK V. S., *Ferroelectrics*, 11 (1994), 162.
[10] BAI F. et al., *Appl. Phys. Lett.*, 86 (2005), 32511.
[11] PRELLIER W., SINGH M. P., MURUGAVEL P., *J. Phys., Condens. Matter*, 17 (2005), R803.
[12] KUBEL F., SCHMID H., *Acta Cryst. B*, 46 (1990), 698.
[13] PALAI R. et al., *Phys. Rev. B*, 77 (2008), 014110.
[14] GUJAR T.P., SHINDE V. R., LOKHANDE C.D., *Mater. Chem. Phys.*, 103 (2007), 142.
[15] FRUTH V. et al., *J. Eur. Ceram. Soc.*, 27 (2007), 937.
[16] CLARK S. J., ROBERTSON J., *Appl. Phys. Lett.*, 90 (2007), 132903.
[17] IHLEFELD J. F. et al., *J. Appl. Phys. Lett.*, 92 (2008), 142908.
[18] XU Y., SHEN M., *Mat. Lett.*, 62 (2008), 3600.
[19] TAUC J. (Ed.), *Amorphous and Liquid Semiconductor*, Plenium Press, New York, 1974, 159.
[20] LEBEUGLE D. et al., *Phys. Rev. B*, 76 (2007), 024116.
[21] SOSNOWSKA I., PETERLIN-NEUMAIER T., STEICHELE E., *J. Phys. C*, 15 (1982), 4835.
[22] SOSNOWSKA I., LOEWENHAUPT M., DAVID W. I. F., *Physica B*, 117 (1992), 180.
[23] JUN LU et al., *Euro. Phys. J. B*, 75 (2010), 451.


*Received 2012-11-22*
*Accepted 2013-09-13*